Simplified Monte Carlo simulations of chemical vapour deposition diamond growth

2009 J. Phys.: Condens. Matter 21 364203

(http://iopscience.iop.org/0953-8984/21/36/364203)

IOP Publishing Journal of Physics: Condensed Matter

J. Phys.: Condens. Matter **21** (2009) 364203 (19pp) doi:10.1088/0953-8984/21/36/364203

Simplified Monte Carlo simulations of chemical vapour deposition diamond growth

Paul W May[1], Neil L Allan[1], Michael N R Ashfold[1], James C Richley[1] and Yuri A Mankelevich[2]

[1] School of Chemistry, University of Bristol, Bristol BS8 1TS, UK
[2] Skobel'tsyn Institute of Nuclear Physics, Moscow State University, Vorob'evy gory, Moscow 119991, Russia

E-mail: paul.may@bris.ac.uk

Received 4 April 2009, in final form 19 May 2009
Published 19 August 2009
Online at stacks.iop.org/JPhysCM/21/364203

Abstract

A simple one-dimensional Monte Carlo model has been developed to simulate the chemical vapour deposition (CVD) of a diamond (100) surface. The model considers adsorption, etching/desorption, lattice incorporation, and surface migration along and across the dimer rows. The top of a step-edge is considered to have an infinite Ehrlich–Schwoebel potential barrier, so that mobile surface species cannot migrate off the edge. The reaction probabilities are taken from experimental or calculated literature values for standard CVD diamond conditions. The criterion used for the critical nucleus needed to form a new layer is considered to be two surface carbon species bonded together, which forms an immobile, unetchable step on the surface. This nucleus can arise from two migrating species meeting, or from direct adsorption of a carbon species next to a migrating species. The analysis includes film growth rate, surface roughness, and the evolving film morphology as a function of varying reaction probabilities. Using standard CVD diamond parameters, the simulations reveal that a smooth film is produced with apparent step-edge growth, with growth rates ($\sim$1 μm h^{-1}) consistent with experiment. The β-scission reaction was incorporated into the model, but was found to have very little effect upon growth rates or film morphology. Renucleation events believed to be due to reactive adsorbates, such as C atoms or CN groups, were modelled by creating random surface defects which form another type of critical nucleus upon which to nucleate a new layer. These were found to increase the growth rate by a factor of $\sim$10 when the conditions were such that the rate-limiting step for growth was new layer formation. For other conditions these surface defects led to layered 'wedding cake' structures or to rough irregular surfaces resembling those seen experimentally during CVD of nanocrystalline diamond.

(Some figures in this article are in colour only in the electronic version)

1. Introduction

Chemical vapour deposition (CVD) of diamond is a maturing technology that is beginning to find commercial applications in electronics, cutting tools, medical coatings and optics [1], and shows great potential for quantum computing [2], biosensing [3], field emission devices and thermionic solar cells [4]. The CVD process involves the gas phase decomposition of a gas mixture containing a small quantity of a hydrocarbon in excess hydrogen [5]. A typical gas mixture uses 1% CH_4 in H_2, and this produces polycrystalline films with grain sizes in the micron or tens of micron range, depending upon growth conditions, substrate properties and growth time. By increasing the ratio of methane in the standard CH_4/H_2 gas mixture from 1% to $\sim$5%, the grain size of the films decreases, and eventually becomes of the order of hundreds down to tens of nanometre. Such nanocrystalline diamond (NCD) films (often termed 'cauliflower' or 'ballas'

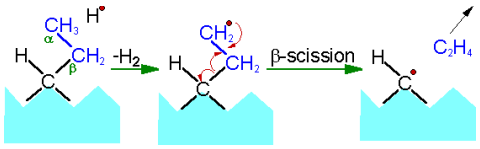

Figure 1. The β-scission reaction thought to remove long-chained hydrocarbons from the growing diamond surface. H abstraction occurs on the upper CH_3 group (designated the α-group), resulting in the bond attaching the β-group to the surface breaking.

diamond) are smoother than the microcrystalline ones, but have larger numbers of grain boundaries that contain substantial graphitic impurities. With further addition of CH_4 the films become graphitic. Diamond films with even smaller grain sizes (∼2–5 nm) are often called 'ultrananocrystalline' diamond (UNCD) films [6, 7]. Most reports of the deposition of UNCD films describe using a microwave (MW) plasma CVD reactor and gas mixture of 1%CH_4 in Ar, usually with addition of 1–5%H_2 [8]. At the other end of the size scale, single crystal diamonds (SCD) up to several carats (1 carat = 0.2 g) in weight have recently been successfully grown in high power MW CVD reactors using 1%–12%CH_4/H_2 mixtures, sometimes with small additions of N_2 or O_2 [9–12].

However, to obtain a diamond film with the desired morphology, electronic and mechanical properties, requires a detailed understanding of the many parameters affecting growth, such as the substrate temperature, gas mixture, process pressure, etc. The difficulty with this, is that even 30 years after diamond CVD was first developed, the exact details of the growth mechanism remain controversial. The so-called 'standard growth mechanism' [13] developed in the early 1990s is a robust description of the general CVD process. In this model, atomic H, created by thermal or electron-impact dissociation of H_2, is the driving force behind all the chemistry. It is generally believed [14] that the main growth species in standard diamond CVD is the CH_3 radical, which adds to the diamond surface following hydrogen abstraction by H atoms. An elevated substrate temperature (typically >700 °C) allows migration of the adsorbed C species until they meet a step-edge and add to the diamond lattice. Another role for the atomic H is to etch back into the gas phase any adsorbed carbon groups that have deposited as non-diamond phases. It is believed that hydrocarbons C_xH_y with 2 or more carbons ($x \geqslant 2$) are prevented from contributing to the growth by the 'β-scission' reaction (see figure 1) which is a rapid, low energy, efficient process that stops the build up of polymer chains on the growing surface. Diamond growth is therefore seen as competition between etching and deposition, with carbons being added to the diamond on an atom-by-atom basis.

This standard growth model has been very successful, and can predict some of the general features of the observed morphology plus growth rates to within an order of magnitude. However, it has problems predicting the crystallite size and whether the resulting film will be UNCD, NCD or even SCD. Some of the basic assumptions of the model have also been called into question. For example, the extent to which the carbon species on the surface are mobile at deposition temperatures between 800 and 1300 K is still controversial. The significance of the β-scission reaction is not known, i.e. just how important is this mechanism in determining the observed smooth faceted morphology? A mechanism for nucleation of a new layer is not incorporated in the standard model. Impurities, such as N_2 in the gas phase, have been suggested as catalysts for nucleation [15], as have larger hydrocarbons, such as C_2H_y or C_3H_y, and defect formation at biradical sites [16].

Our group recently developed a modified version of the standard growth model which considers the effects of all the C_1 hydrocarbon radicals (CH_3, CH_2, CH and C atoms) on both monoradical and biradical sites on a (100) diamond surface [17]. In this model, for most standard deposition conditions (i.e. with high atomic H concentrations at the growth surface) diamond growth is still dominated by CH_3 adding to monoradical surface sites, leading to large crystals. Addition of CH_3 to the biradical sites also leads to large crystals, since the unused surface dangling bond is rapidly hydrogenated during the process of converting the CH_3 adduct into a CH_2 surface group [18]. However, the increased relative contribution of the biradical mechanism enhances the probability that other reactive hydrocarbon species (C_2, C_2H, etc) from the gas can add to these biradical sites. Such reactive species then have the opportunity to cross-link on the surface, creating a strongly-bonded (maybe even non-etchable) defect. This surface defect could act as either a renucleation point for a new epitaxial layer, or, if it is misaligned with the existing lattice, a new crystallite growing in a different direction to that of the main bulk. This last possibility is often termed 'renucleation', and leads to a decrease in the average crystal size. If renucleation occurs frequently, the crystallite size can drop from mm to μm, and eventually to nm, and the films are termed SCD, MCD and (U)NCD accordingly.

As well as CH_3, addition of the other less abundant but highly reactive C_1 species, particularly atomic C, to either type of radical site at high H atom concentration, can also be a route to growth, since the dangling bonds on the adduct would be readily hydrogenated converting the adduct into CH_2. However, at low H atom concentration, the dangling bonds on the adduct can cross-link to lattice sites, again leading to renucleation and subsequent smaller crystal sizes. Additionally, evidence from very recent quantum-mechanical *ab initio* modelling [19] shows that some C_1 species, in particular C atoms, can directly insert into the C–H surface bonds of diamond with a low or even zero energy barrier. This may be yet another mechanism to create surface defects.

This model also relies upon surface migration of CH_2 groups along and across the reconstructed dimer rows in order to predict growth rates to within a factor of two of experimental observations. In the model we derived equations for the fraction of monoradical sites, R, and biradical sites, R^2, based upon the substrate temperature, T_s, and the concentrations of H and H_2 above the surface. Under typical CVD diamond conditions with $T_s \sim 900$ °C and 1%CH_4/H_2, $R \sim 0.1$, ∼10% of the surface carbon atoms support monoradical sites, and 1% have biradical sites. The model also derived an expression for the average crystallite size $\langle d \rangle$ which depends upon T_s and crucially upon the square of the ratio of the atomic

H concentration to that of the sum of the C_1 hydrocarbon concentrations, i.e. $([H]/\Sigma[CH_y])^2$, where $y \leqslant 3$. The expression for $\langle d \rangle$ predicted values that agreed closely with experiment that ranged from a few nm corresponding to UNCD [20] to mm for single crystal diamond [21].

Despite these successes, evidence for surface migration, nucleation processes, the effects of gas impurities and gas-surface reactions are sparse and mostly circumstantial. In this paper we shall describe the use of a simplified Monte Carlo like program to simulate diamond growth on the (100) surface in an attempt to gain an insight into each of these processes. Before we describe our approach, we shall explain in more detail the background to each of these problems.

1.1. Surface migration, and Monte Carlo modelling

Experimentally, there are numerous papers describing apparent step-edge growth of diamond during CVD. For example, Lee and Badzian [22] found that following epitaxial MW CVD, hillock growth occurred through two-dimensional nucleation on terraces when the density of surface steps was low, while step-flow growth proceeded along the (110) directions when there was a high density of steps. They also found that the growth mechanism changed with gas phase CH_4 concentration: for low $[CH_4]$ they observed step-flow growth, for medium $[CH_4]$ hillocks appeared, and for high $[CH_4]$ the growth became random. Growth experiments by other workers [23] using off-angle Ib diamond substrates also suggested that step-growth was occurring upon the (100) surface, resulting in the formation of large terraces of (2×1) reconstructed diamond. These and many other reports provide evidence that a growth species adsorbs upon the diamond surface and subsequently diffuses across the growing surface to step-edges and/or other adsorbed atoms, whereupon it adds to the lattice.

For metals, diffusion of atoms across the surface is known to be an essential part of the growth dynamics [24]. However, for diamond the main growth species are not atoms but CH_3 radicals, and the surface is covered with H atoms which repel both incoming gaseous precursors as well as migrating adsorbates. The high deposition temperatures lead to short lifetimes for physisorbed species, thus only chemisorbed groups need be considered capable of migrating. Chemisorbed molecular groups, such as CH_2, can, in principle, migrate along or across a dimer row so long as they have an adjacent empty site to move into. These empty sites are created by H abstraction reactions. Therefore the migration process can be considered to be mediated by the local atomic H concentration since this determines the availability of empty sites. Such *chemical migration* has been considered by a number of groups [18, 23, 25–29], and the estimated migration length of ~10 Å [27] is consistent with the experimentally observed terrace sizes [30]. A combination of chemical migration, etching and insertion reactions has been used to give a broad explanation for some of the observed morphological patterns of diamond growth, such as lateral propagation of lattice steps, and different plane textures [26, 27, 31].

Due to the difficulties of obtaining direct evidence for surface migration by experimental means, various workers have used theoretical models to try to calculate if such migration is feasible, and what effects it might have upon morphology. A common approach is that of kinetic Monte Carlo (KMC) simulations. In these, a model of the diamond surface is created and a set of relevant processes and mechanisms are constructed, including those in which C species (CH_3, C_2H_2, etc) are allowed to strike the surface randomly with a certain impact rate. Some of these will adsorb with a probability given by the rates known from experiment. The KMC simulations show that migration then occurs, with the probability of the C species jumping to the next site being governed by an activation barrier and the surface temperature. When the C species meets a step-edge, the species may bond to the edge thereby propagating the lattice, with a probability given by the results of detailed calculations previously carried out based upon modelling the geometry, steric effects, and kinetic data. Given sufficient numbers of impinging methyls and sufficient computing time many layers of diamond growth can be built up.

Early kinetic models of CVD diamond growth [32–35] predicted the experimentally observed growth rates but were unable to reproduce some aspects of the morphology, such as the appearance of dimer rows. This is because a major limitation of KMC methods is that they assume advance knowledge of the rates of all the relevant mechanisms. Later KMC models [36–43] became far more detailed, and began to reproduce many of the experimentally observed features. One of the best and most recent KMC implementations is that of Netto and Frenklach [44], which used methyl radicals as the only growth species, with the incorporation into the diamond surface described by means of a ring-opening/closing mechanism. CH_2 migration along and across the dimer reconstructions was included, as well as the reforming of dimer-reconstructed bonds from two suitable adjacent surface radical sites. Etching was only considered to occur at isolated incorporated CH_2 groups (described by the reverse of the ring-opening/closing mechanism) and reconstructed dimers (by a one- or two-carbon-removal process). The energetics and kinetic data for these reactions were sourced from numerous calculations and experimental measurements. Overall, the Netto–Frenklach model suggested that CH_3 can randomly adsorb upon a diamond surface and then migrate until multiple species coalesce. During this process, the substrate surface can act as a template for migrating species to form new dimer reconstructions and, in combination with etching, results in the smooth surface growth observed.

Cheesman [28] recently used a combination of quantum-mechanical and molecular-mechanical methods to reinvestigate some of the previous carbon migration studies. The carbon migration pathways studied were those first proposed by Frenklach and Skokov [27] and involved the movement of species along and across the dimer rows present upon the (100) diamond surface. His studies confirmed the feasibility of these carbon migration reactions. The overall effective activation energy and thermodynamic data suggest that migration of CH_2 upon a pristine diamond surface occurs more readily than previously reported, as many of the key reaction steps have a reduced or no activation energy.

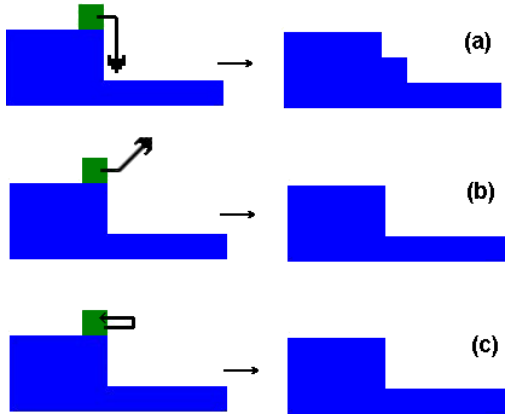

Figure 2. Schematic diagram showing the possible fates for a migrating C species (shown as a green block) when it encounters the top of a step-edge. (a) 'Lemmings'—the species drops to the bottom layer of the step and then adds to the lattice. (b) 'Eagles'—on attempting to go down the step, desorption occurs. (c) 'Cowards'—the potential barrier to drop down the step is too great and the species remains where it is.

1.2. Migration down a step-edge

Processes not included properly in any Monte Carlo model to date are those which can occur when a migrating carbon species meets the top of a step-edge, see figure 2. There are three possibilities: (i) the species simply drops (migrates) down to the bottom of the step-edge (which may be more than one atomic layer deep) and adds to the lattice there; (ii) on attempting to go down the step, enough bonds are broken that it desorbs back into the gas phase; or (iii) it does not drop down but stays where it is and subsequently migrates back away from the edge [45]. These three possibilities (which we have somewhat light-heartedly termed 'lemmings', 'eagles', and 'cowards', respectively), are governed by the Ehrlich–Schwoebel potential (ESP), which is the barrier (positive, negative or zero) which an edge species must overcome to fall down a step-edge [46, 47]. 'Lemmings' occur with a zero, negative or small positive ESP, while 'cowards' correspond to an infinite positive ESP. 'Eagles' would occur with a zero or positive ESP. Which of these three processes is dominant in diamond growth is arguable, and detailed *ab initio* calculations would be required to resolve this issue. However, in section 2 we shall argue from a geometrical point of view that 'cowards' are the best description for diamond.

1.3. Nucleation of a new layer

An isolated CH_3 group adsorbed onto a pristine (100) diamond surface has a number of possible fates. It can migrate across the surface, hopping along and across the dimer rows in the form of a bridging CH_2, as discussed in 1.1 above. But on a pristine surface there are no step-edges to which it can attach, and so this migration will occur until it eventually desorbs or is etched back into the gas phase. An alternative fate is possible if the migrating C species encounters a second C species which is also migrating randomly across the surface—a process akin to a Langmuir–Hinshelwood (LH) mechanism [48]. Alternatively, the second C species can adsorb immediately on a site adjacent to the one currently occupied by the first C, which would be analogous to an Eley–Rideal (ER) type process [48]. In either case, the first C species now has the opportunity to react with its new neighbour, forming an adsorbed 2-carbon unit which would be much less mobile than either of the two C_1 monomers. Such a relatively static unit could form the basis for the nucleation of a new layer, as other migrating C species would now have an effective 'step-edge' upon which to attach. The effectiveness of this as a nucleation site would depend upon the relative rates of migration of other C species towards the unit (combined with the probability of attachment once they meet), compared to etching/desorption/dissociation rate of the 2-carbon unit which would remove the nucleation site. Once three or more carbons are added to this nucleus, etching/dissociation becomes less and less likely, and the new layer would progress rapidly. The 1D Monte Carlo model (described in section 2) assumes that the so-called *critical nucleus* (the minimum number of blocks that become immobile and unetchable, and which cannot dissociate [45]) is only 2 blocks. We note that this is a simplification, since for nucleation on 2 dimensions, as on a real diamond surface, this critical nucleus may be as high as four carbons [15]. The rate of LH nucleation would depend upon the migration rate, and hence crucially upon the surface temperature. The rate of ER nucleation would also vary with the surface temperature, but more critically upon the rate of CH_3 adsorption, and thus be sensitive to the gas conditions above the surface.

Yet another possible fate for the original migrating C species is the formation of an immobile surface defect if the multiple bond-breaking and bond-reforming processes that occur during each migration step [28] go awry. This can happen, for example, as a result of H abstraction converting the benign migrating CH_2 group into a more reactive CH or atomic C moiety. Most of these isolated surface defects would probably be etched back into the gas phase, leaving behind a pristine diamond surface. But some may survive long enough to act as a nucleating point for a new layer, which may or may not follow the orientation of the underlying lattice.

Similar static surface defects could also be formed when CH_3 adds to the less abundant ($\sim$1% of the surface) *bi*radical sites, since the resulting adduct will find itself with a reactive dangling bond immediately adjacent to it. The most likely fate for this dangling bond is to be rapidly hydrogen terminated by reaction with the abundant gas phase atomic H. However, an alternative pathway is for a reactive gas phase species such as C_2, C_2H, C, etc, to add to this dangling bond and then reconstruct into a surface defect. Although this may be a minority process due to the low abundance of these species, every time it occurs it can create a renucleation point, leading to a decrease in the average crystallite size [17].

Another defect-forming process involves adsorbing unsaturated atomic C or CH species, since their 'dangling bonds' permit unusual surface bonding. For standard diamond CVD conditions, the concentrations of C and CH striking the surface are usually negligible compared to that of CH_3. But under H-poor conditions, such as those used for UNCD growth, they can

become significant contributors to the growth [49]. A further possibility for initiating a new layer from a static surface defect is from impurities in the gas phase, such as N_2 (see 1.4 below). By whichever mechanism they are created, such static surface defects could act as the critical nucleus needed to help start a new layer, or instigate the (re)nucleation of a new crystallite, ultimately leading to a polycrystalline film.

1.4. Nitrogen additions

The presence of even trace amounts of N_2 in the gas mixture strongly affects diamond growth, increasing the growth rate by a factor of around 2 and giving the surface morphology a more pronounced (100) texture [50, 51]. For larger N_2 concentrations, the grain size decreases and the film becomes nanocrystalline [52]. This is usually explained by an increase in secondary nucleation and a higher concentration of non-diamond carbon in the film (particularly at the grain boundaries). However, despite these large effects, the amount of N incorporated into the diamond lattice is usually in the ppm range, which is several orders of magnitude below the N/C ratios in the gas phase [53]. This led to the suggestion that the N must be acting as a catalyst for surface reactions. Butler and Oleynik [15] proposed that N_2 in the gas phase would be converted to CN, which would then adsorb onto the (111) surface. Since CN cannot undergo a β-scission type reaction, it cannot easily be removed from the surface, and will remain there acting as a nucleation point for the start of a new layer. If the growth conditions are such that nucleation of the new layer is the rate-limiting step, small quantities of adsorbed CN would greatly increase the growth rate, while giving a very low N incorporation level (the lower limit being only one N needed per atomic layer). While this may be true for the (111) surface, it is not straightforward to use the same explanation for the (100) surface. Another explanation for the role of N is that the lattice distortions associated with the incorporation of substitutional nitrogen affect the energetics and rates of CH_3 adsorption onto nearby surface sites [54].

1.5. Limitations of previous KMC models

One of the limitations of the KMC simulations of diamond growth so far reported in the literature is the computational expense of the long simulation runs required. The models of the diamond surface have usually been very detailed, involving the full 3D geometry of the various surface structures at the atomic scale, plus the orientation of the incoming and adsorbed C species—of which there can be several types. They also involve estimates (some accurate, some little more than educated guesses) for the rates of all the various reactions and their temperature-dependent Arrhenius parameters. Many of the essential kinetic parameters, such as activation barriers for migration and pre-exponential factors are not known with any precision (if at all), and even the identity and concentrations of the species striking the surface are still poorly known. KMC is particularly problematic for diamond growth, since the majority of impacts of gas phase species with the mostly inert H-terminated surface will result in the species bouncing off, with no net growth or etching. Thus, a great deal of computational time is wasted on non-events. The KMC models in the literature, therefore, often require many days of computing time to simulate the addition of only a few carbons to the lattice. The advent of faster computers has helped this situation somewhat, but a simplified approach is still needed if insights into 'the big picture' are to be obtained in reasonable timescales [55]. In this paper we describe such a simplified approach—the aim being to devise the simplest Monte Carlo model for diamond growth we can—which can model the growth of hundreds of layers of (100) diamond in only a few hours—yet which still maintains a physical correspondence to the real-world process.

2. The Monte Carlo model

One requirement for our model was that we wished to be able to view the growth of the diamond surface in real time using a desktop PC. The program was written using Microsoft QuickBasic, which although not optimized for modern PCs, was easy to program and had the required graphical capability built in.

2.1. The basic model

In many respects our model resembles the standard 1D KMC models used to model crystal growth and thin film molecular beam epitaxy (MBE) for a decade or more [45]. However, our version contains a number of parameters specific to diamond growth, as well as several unique subroutines written specially to test diamond-growth-specific mechanisms, such as β-scission.

In our simplified 1D Monte Carlo model, the diamond lattice is represented in only 2 dimensions, as a cross-section, with the growing (100) surface positioned towards the top of the screen. Each C atom is represented by a square block within the lattice, with different coloured blocks representing different 'types' of carbon bonding. Carbons fully bonded into the diamond lattice are coloured dark-blue. Carbons temporarily adsorbed on the surface are green, and carbons that have formed an immobile surface defect (see 1.3, above) are coloured black if the defect formed following direct impact from an incoming block, or brown if the defect formed following a migration step.

The grid has a maximum size of 600 × 400, but for speed of computation 2 × 2 blocks were used for most simulations, making the effective grid size 300 × 200. At the start of the program, a flat horizontal surface of dark-blue blocks is defined at the bottom of the screen to represent a single crystal diamond substrate. A random number, R_1, is then generated and compared to the probability of a new incoming block, P_{new}, which is calculated based on the known flux of CH_3 radicals towards the surface under typical CVD conditions (see section 2.2). If $R_1 < P_{\text{new}}$ a new incoming green-coloured block is chosen at a random horizontal position at the top of the screen, and then allowed to drop vertically until it meets the surface whereupon it temporarily adsorbs at this position. (Readers familiar with computer games may recognize the similarities between this model and the arcade game 'Tetris'.)

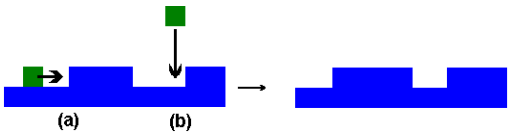

Figure 3. The model for (a) Langmuir–Hinshelwood-type and (b) Eley–Rideal-type step-edge growth.

This block represents a generic C_1 adsorbing unit, which is most probably CH_3 but could be species such as C, CH, CH_2 or even CN. The adsorbed green block then has a number of possibilities, depending upon the local morphology where it landed, and each possible fate is tested sequentially at every time-step of the program.

A block landing immediately adjacent to another block of any colour either to its left, right or both, is considered to undergo direct ER-type growth (see section 1.3 and figure 3). The block is coloured dark-blue and bonds to its neighbour, and remains there for the duration of the program. In this model, the diamond lattice itself (blue blocks) is considered unetchable, so once a moving block has added to the lattice, it cannot subsequently be removed (except in the special case of a β-scission reaction, see section 3.3).

Alternatively, if the initial green block lands in a position with no blocks either to its left or right, the block can simply desorb (or be etched) back into the gas phase. Another random number, R_2, is generated and compared with the probability of desorption/etching, P_{desorb} (see section 2.2). If $R_2 < P_{\text{desorb}}$ the block desorbs and is removed. If the block remains on the surface, another possible fate for it is to stick permanently to form a static, unetchable defect (see section 1.3). A third random number R_3 is generated and compared with the probability for direct–defect formation, $P_{\text{dir-def}}$. If $R_3 < P_{\text{dir-def}}$ the block is coloured black and attaches permanently to the lattice. If the block does not add to the lattice, desorb or permanently stick as a defect, then a final possibility is that it migrates. A fourth random number, R_4, is generated and compared to the probability of migration, P_{mig} (see later). If $R_4 < P_{\text{mig}}$ the block will jump left or right one space, with equal chance. If this block now finds itself next to another block of any colour, it will permanently bond to it and turn dark-blue. This is analogous to the LH model for growth (see section 1.3 and figure 3). But if the block still finds itself with no neighbours in its new position, it might form a static defect (with probability $P_{\text{jump-def}}$) in which case it is coloured brown, or remain temporarily adsorbed, ready to migrate again at the next time-step. $P_{\text{jump-def}}$ can be different from $P_{\text{dir-def}}$ since the mechanisms forming the static surface defect might be different in each case.

There are two special cases that need to be considered. First, β-scission can be modelled by scanning the surface blocks after every time-step and identifying and deleting any 2-block pillars that may have arisen as a result of blocks landing or migrating (see figure 4). The probability that β-scission occurs, thereby deleting any individual 2-block pillar, is given by P_{beta}. This can, in principle, be estimated from known reaction rates, but, in practice, is chosen to be either 0 (β-scission never happens) or 1 (β-scission happens every time it is possible at each time-step).

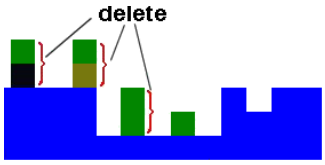

Figure 4. The model for β-scission. All isolated 2-block pillars are deleted with probability P_{beta}. Examples of 2-block pillars that would be deleted are (from left to right) green-on-black, green-on-brown and green-on-green. Green-on-dark-blue (not shown) is another type of pillar that would be removed.

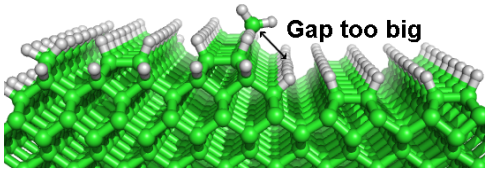

Figure 5. Diagram of a migrating CH_2 group attempting to drop down a step-edge on the (100) surface calculated using density functional theory. The gap is too large, and so the CH_2 cannot move this way ('lemmings' cannot occur).

Second, there is the issue of blocks migrating off the top of step-edges (see section 1.2). Preliminary DFT calculations show that the probability of a migrating CH_2 group desorbing is not significantly different at the top of a (100) step-edge to that found anywhere else on the surface. This makes the 'eagles' scenario unlikely. Furthermore, the distance between the top and bottom of a step on the (100) diamond surface is too great to allow a migrating CH_2 group to bridge the gap (see figure 5). Hence, the ESP is effectively infinitely large, eliminating the 'lemmings' scenario as a plausible choice. Thus, we have adopted the 'cowards' scenario as the default process, and this choice leads directly to some of the surface morphologies that are predicted (see section 3.1).

The program is cycled until it is stopped manually or until a set number of layers (typically 150 to provide statistical invariance) have grown, at which point the data are saved. Depending upon the choice of probabilities for the various events, the program can take from an hour to several hours to grow 150 layers (on a Pentium 4 PC). Thus, the evolution of the surface morphology can be directly viewed on the computer screen, giving insight into which parameters control different aspects of growth.

2.2. Choosing the probabilities and time-step

In a Monte Carlo model of this type, the time-step is chosen to be equal to, or faster than, the fastest process occurring. This fastest process (which turns out to be surface migration) is normalized to give a probability of 1 (or less if required) to occur at each time-step, and the other processes are assigned probabilities based on their relative rates with respect to this fastest one. In order to simplify matters, we shall assume that the growth conditions are fixed for standard polycrystalline CVD grown at a substrate temperature of ~900 °C [17]. The first process to consider is the impact rate of CH_3 species on the surface. We shall assume that CH_3 is the only species

important for growth of diamond, and thus we require the flux of CH_3 striking the surface. The concentration of CH_3 close to the surface has been calculated [7] from a model of the gas phase chemistry to be $[CH_3]_s \sim 10^{13}$ cm^{-3}. Thus, the number of CH_3 impacts cm^{-2} s^{-1} is given by $[CH_3]_s \times v/4$, where v is the mean gas speed which is proportional to the square-root of the gas temperature close to the surface. This temperature of $T_{ns} \sim 1200$ K results in a CH_3 flux of $\sim 3.2 \times 10^{17}$ impacts cm^{-2} s^{-1}. From the C–C bond length in diamond we can calculate that 1 cm^2 of the surface contains $\sim 1.56 \times 10^{15}$ C atoms. Thus, each C atom on the surface is struck by an incoming CH_3 radical $3.2 \times 10^{17}/1.56 \times 10^{15} \sim 200$ times s^{-1}. However, most of these impacts will be with a hydrogenated surface C, and so the CH_3 will simply bounce off. Only those impacts which strike dangling bonds will be important for growth and need be considered in the model. For standard CVD conditions (with substrate temperature $\sim$900 °C), $\sim$10% of the surface carbons have a dangling bond (see section 1). The probability of adsorption onto a radical site is $\sim$0.4 [20]. Therefore, the impact rate for CH_3 leading to adsorption will be $\sim$8 s^{-1} per radical site.

The migration rate to be considered is that for a CH_2 bridging group to move along or across a dimer row. The rate constants for these two processes have been estimated [18, 23, 44] to be identical and equal to $\sim 1.5 \times 10^7$ s^{-1} (at $T_s = 900$ °C), from which, to obtain a rate, we have to multiply by 0.1 since migration is only possible if there is an adjacent radical site ($\sim$10% of the surface sites for diamond CVD standard conditions) upon which to jump. Thus, the migration rate for our model is 1.5×10^6 s^{-1}. This could be an underestimate since Cheesman's more recent calculations suggest the migration rates may have lower barriers and so a factor of $\sim$10 faster. Nevertheless, taking the lower value (to minimize computer time) it is clear that surface migration processes are nearly 200 000× faster than the impact rate.

The desorption rate is a crucial parameter, and in our case no distinction is made between desorption and etching—the probability of removal of an isolated carbon species from the surface is considered to be controlled by a single parameter, P_{desorb}. The exact mechanism by which this etching occurs is controversial, because, based upon thermodynamic considerations, most of the proposed carbon-removal reactions (except β-scission) from a pristine (100) diamond surface would appear to be too slow [29, 56]. However, carbon-removal studies, looking at the effects of hydrogen atom etching upon a diamond surface, show that etching does indeed occur, and that methane is the predominant carbon-containing species etched [57]. To obtain a value for P_{desorb} we follow Netto and Frenklach [44] and assume that the desorption/etching step is simply the reverse of the CH_3 addition process—here an adsorbed CH_2 group is removed back into the gas phase (catalyzed by H) as CH_3, leaving behind a surface dangling bond. The rate of this process depends upon the local geometry of the CH_2 group on the surface, and upon which type of radical site is created. For the two types of bridging site (termed A3 and A4 in [18, 27]), the rates are estimated to be 1.5×10^5 and 5100 s^{-1}, respectively. Since these two sites should have equal abundance and probability of occurring (especially under conditions with high [H] and therefore fast H abstraction rates), an average of these two rates has been taken as $\sim$77 550 s^{-1}. Due to the uncertainty in this value and the possible controversy over its origin, P_{desorb} is a parameter which we shall vary over a wide range to determine its effects (see section 3.2).

The rate of formation of static surface defects is more difficult to estimate. We assume that these defects are formed from adsorption of reactive C_1 species or from trace impurities such as N_2 (or CN derived from it). Under typical CVD diamond conditions, the concentration of C_1 species at the growing surface is usually <1% of that of CH_3 [7], and if all of these caused a surface defect the rate would be 0.01× that of the CH_3 impact rate, i.e. 0.08 s^{-1} per radical site. However, only a small percentage of these C_1 impacts would create surface defects—the remainder would probably form non-diamond carbon and be rapidly etched away. Unless special care is taken to remove all traces of nitrogen from the CVD system, N_2 is usually present in the gas mixture as an unwanted impurity in trace amounts of $\sim$10–100 ppm of the total gas. For a nominally 1%CH_4/H_2 gas mixture, the concentration of N_2 therefore corresponds to $\sim$0.1–1% of that of CH_4. Thus we can estimate that the impact rate of N-containing species with the surface will be comparable with that of the C_1 species, and most of these impacts will contribute to defect formation since they cannot be removed via a β-scission mechanism (see section 1.4). With no literature data upon which to base further estimates, we have chosen a value of $\sim$10% of the C_1 impacts together with 100% of the N-containing species to jointly cause surface defects, giving a default rate of 0.016 s^{-1}.

Furthermore, a migrating CH_2 group is assumed to 'attempt' to migrate every time-step, and this involves the breaking of one of the bonds joining it to the lattice catalyzed by H abstraction. When this bond reforms, it can either do so in the same place (i.e. the CH_2 group stays where it is), or it can join to a neighbouring C (migration). In either case, the bond-reforming process has a probability of 'going wrong', creating a surface defect either in the original or new position for the species, respectively. With no literature data, the value 0.016 s^{-1} has also been used for the rate at which a migrating CH_2 group bonds in a defective manner. Although the values chosen for rate of formation of the two types of surface defect seem somewhat arbitrary, we shall investigate the effect of varying them to ascertain the sensitivity of the findings to the chosen values. As such, they serve to highlight the lack of reliable data in the literature for these fundamental processes, and present it as a challenge to theoreticians to calculate these values more accurately.

Normalizing these values to the fastest process, migration, we obtain the probabilities for each process occurring per time-step given in table 1. The maximum growth rate will occur when there is 100% utilization of all the incoming C species and no loss mechanisms (no desorption or β-scission). At an impact rate of 8 s^{-1} per radical site and a C–C bond length of 1.5 Å we obtain that the maximum growth rate for typical diamond deposition conditions is $\sim$4.3 μm h^{-1}. This agrees quite well in magnitude with experimental values, which will be less than this due to the loss mechanisms.

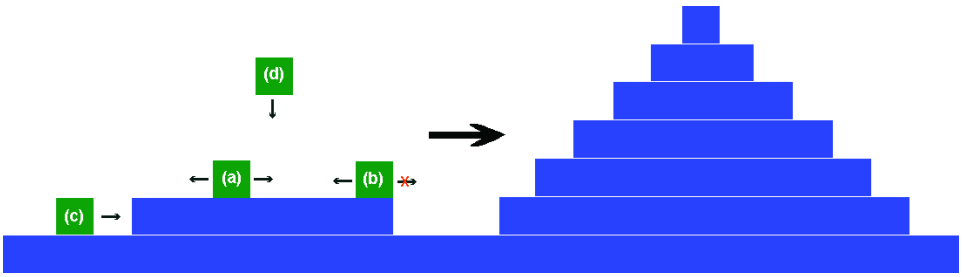

Figure 6. Schematic diagram of how the 'cowards' scenario can lead to the 'wedding cake' structure. Blocks (a) and (b) are trapped on the top of a mesa structure and cannot drop down to the lower level, but they can migrate along the length of the mesa, where they may meet and form a critical nucleus. Blocks already on the lower level such as (c) can migrate and stick to the step-edge, while gas phase blocks (d) can adsorb onto the upper and lower levels. If the desorption rate is low, and the rate of (d) is relatively fast so that adsorption on the top layer occurs before the lower level is complete, then the relative probabilities for each process leads to the formation of a regular pattern of tapering stacks of islands upon islands, reminiscent of a wedding cake [55].

Table 1. The rates per site and the normalized probabilities per time-step for each of the processes in the model.

Process	Rate s^{-1}	Probability symbol	Normalized probability
Surface migration along and across (100) dimer rows	1.5×10^6	P_{mig}	1
CH_3 impact on radical site	8	P_{new}	5×10^{-6}
Desorption/etching	77 550	P_{desorb}	0.05
Surface defect creation following direct impact	0.016	$P_{\text{dir-def}}$	0.0005
Surface defect creation following migration	0.016	$P_{\text{jump-def}}$	0.0005
Combined surface defect creation (renucleation)	0.016	P_{renucl}	0.0005
β-scission (taken to be the same as that of migration, i.e. it happens at every time-step)	(1.5×10^6)	P_{beta}	1
Addition of a migrating C group to a step-edge	—	$P_{\text{add-step}}$	1

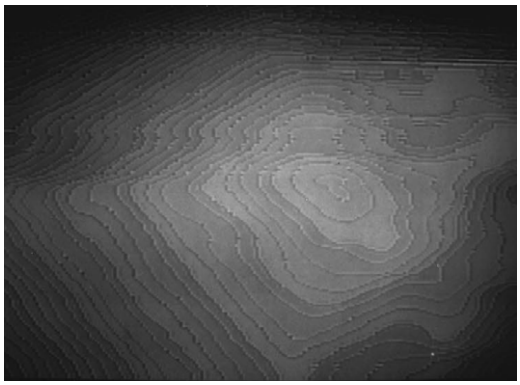

Figure 7. Scanning probe microscope image (size ~1000 × 600 Å) of (100) diamond facets following CVD, exhibiting layered growth with near-atomic steps and the presence of pyramidal features (the wedding cake structure). Reprinted with permission from [59]. Copyright 1997, American Institute of Physics.

3. Results

Using the values given in table 1, the program achieved its goals of simulating the growth of 150 layers of diamond in around 2 h, with the morphology evolving on the screen in real time. Visually, the film appeared to grow from the step-edges, as a result of both migration and direct Eley–Rideal processes. The type of growth seen, the growth rate and the film morphology were a complicated function of the probabilities used. We shall look at the effect of each of these in turn.

3.1. Lemmings, eagles or cowards?

We shall first examine the validity of the choice of 'cowards' as the default strategy for migrating blocks approaching the top of a step-edge. The program was modified to allow the possibility of each of the three strategies in turn, and the results compared. For 'lemmings', the blocks were allowed to jump off the step-edge and fall vertically down (which may be more than one layer deep) until they met the bottom of the step, at which point they attached at the corner and became part of the diamond lattice. For 'eagles', any blocks attempting to move over a step-edge were assumed to have desorbed and so were removed from the program. When 'coward'-blocks attempted to move off the top of a step-edge, they would remain where they were (with a small possibility of forming a surface defect there). Thus, 'coward'-blocks would often become trapped on the top of mesa structures, with no pathway to escape, except desorption. If the desorption rate was low, then eventually a second layer would form as two migrating 'coward'-blocks trapped on the mesa would meet and form a critical nucleus. This led to the development of layered 'wedding cake' structures [55, 58], as shown in figure 6. Growth morphologies very similar to this have been seen experimentally. For example, figure 7 shows layered growth and near-atomic steps on the (100) surface of diamond following CVD [59], suggesting that the wedding cake model for growth is realistic for some growth conditions.

The program was executed with each of the three scenarios, and for both high and low desorption rates, and the results can be seen in figure 8. For the standard (relatively high) value of P_{desorb} (0.05), figure 8(a) shows that the growth rates are very similar for all three scenarios, as are the surface roughness values (figure 8(b)). Thus, for the standard diamond

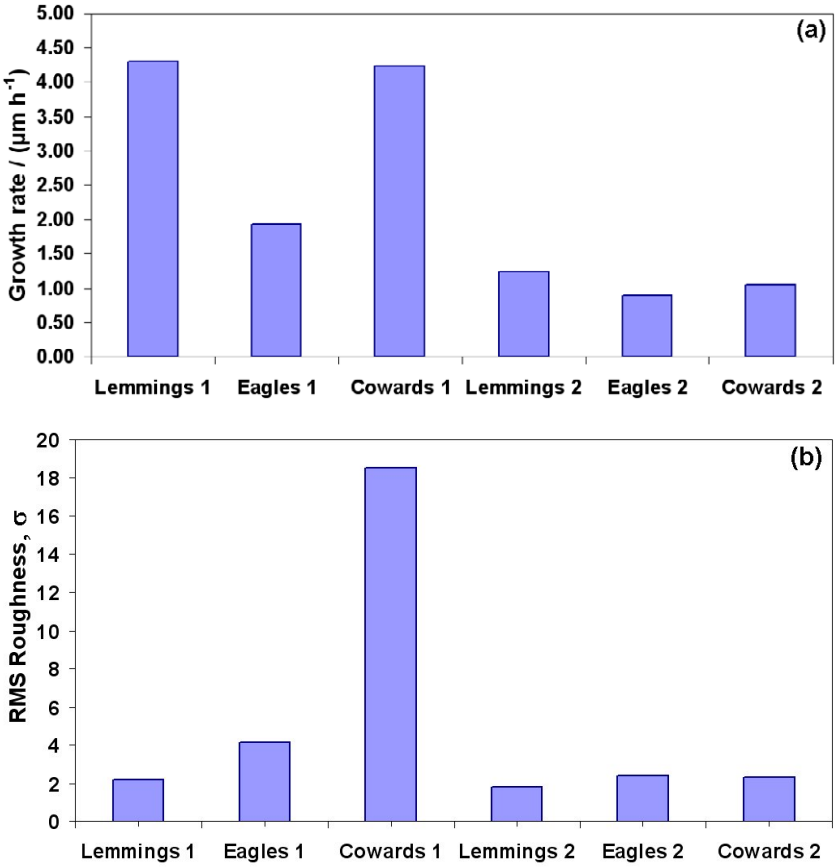

Figure 8. (a) Growth rate and (b) RMS roughness (in blocks, where 1 block = 1 C–C bond length ∼1.5 Å) comparison between the three scenarios for migration off a top step-edge, using (1) $P_{\text{desorb}} = 0.000\,15$ and (2) $P_{\text{desorb}} = 0.05$ (standard value), and with β-scission turned off ($P_{\text{beta}} = 0$).

growth conditions, the results of the growth simulation are relatively insensitive to the choice of scenario. However, for a P_{desorb} value (0.000 15) much smaller than standard, such as may occur at very low substrate temperatures, there is a marked difference between the three scenarios. The growth rates for 'lemmings' and 'cowards' are similar, and close to the maximum growth rate for 100% carbon utilization. But the growth rate for 'eagles' is much smaller, as the effective overall probability of desorption/etching is significantly increased because *all* blocks encountering a top step-edge desorb. The major difference between the scenarios at this low P_{desorb}, however, is in the film roughness. 'Lemmings' and 'eagles' produce relatively flat films, since in the former case all voids and cavities are quickly filled by blocks dropping down into the layer below, and in the latter case because most trapped mesa blocks desorb at the edges before nucleating a second layer. The default scenario of 'cowards', however, produces extremely rough, spiky surfaces upon an underlying 'wedding cake' structure. Such spiky surfaces have never been reported in diamond CVD, probably because the P_{desorb} values used in the simulation are unrealistic for real growth.

3.2. Effect of P_{desorb}

The relative probability of desorption/etching is a crucial parameter. For the standard conditions given in table 1, except with β-scission turned off and with migration turned on ($P_{\text{mig}} = 0.67$ per time-step, appropriate for equal probability of hopping left, right, or staying in place), we obtain the upper curve in figure 9. At $P_{\text{desorb}} = 0$, there is no mechanism to remove blocks from the lattice, so the C utilization rate is 100% and we see the maximum growth rate of 4.3 μm h^{-1}.

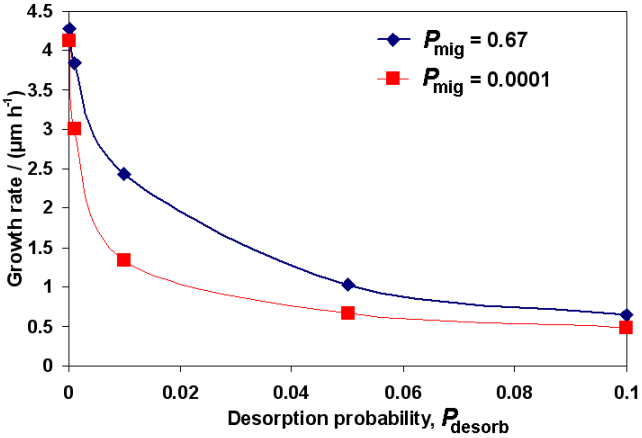

Figure 9. The calculated diamond growth rate as a function of P_{desorb} (with β-scission turned off, $P_{\text{beta}} = 0$), for two values of migration probability, and the standard conditions in table 1.

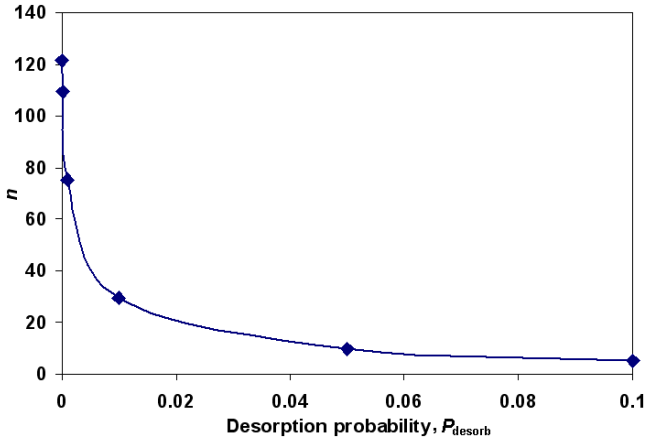

Figure 10. The calculated average number of jumps, n, made by the adsorbing blocks as a function of P_{desorb} (with β-scission turned off, $P_{\text{beta}} = 0$) and the standard conditions in table 1.

Conversely, when $P_{\text{desorb}} = 1$ all the blocks will desorb as soon as they land leading to a growth rate of zero. Between these two values we obtain a smooth curve, with a predicted growth rate of $\sim$1 μm h^{-1} for the standard P_{desorb} value of 0.05. This is in very good agreement with the experimental growth rates found in a hot filament reactor under typical CVD conditions [49]. The lower curve in figure 9 is for the same conditions except with migration almost completely turned off ($P_{\text{mig}} = 0.0001$). The limiting values for $P_{\text{desorb}} = 0$ and 1 are identical in both curves, since migration should not affect these points. The remainder of the curve is slightly lower, showing that turning off migration decreases the growth rate. The surprising finding is that migration only appears to increase the growth rate by a factor of 2 at most, which somewhat smaller than the factor of $\sim$10 reported by Netto and Frenklach [44].

The mean number of jumps made by an adsorbed species, n, as a function of P_{desorb} has been calculated by the program and is shown in figure 10. For standard diamond CVD conditions, $n \sim 10$ jumps, which means that each adsorbed species ends up, on average, $\sqrt{10} \sim 3$–4 sites away from its landing space. $\sqrt{n}$ is sometimes called the *surface diffusion length*, ℓ_s, [45], and can be approximated by the expression

$$\ell_s \sim (D/F)^{1/6} \tag{1}$$

where D is the surface diffusion constant and F is the impact rate per site s^{-1}. F is known from table 1, and for a one-dimensional random walk [58],

$$D \sim d^2 v/2 \tag{2}$$

where d is the mean distance covered in a single jump (=1 site) and v is the migration rate (also given in table 1). Therefore, $D \sim 7.5 \times 10^5$ s^{-1}, and $\ell_s \sim 7$ sites, which is similar to the value of 3–4 obtained by the program.

The value of n relates directly to the small increase in growth rate seen in figure 9, as well as to the observed growth morphology. For the typical CVD diamond conditions given in table 1 (with $P_{\text{desorb}} = 0.05$), the observed morphology is smooth, with an RMS roughness of $\sim$1.5 blocks, (see figure 11), and step-edge growth was observed. In contrast, when decreasing P_{desorb} to 0.005, layered structures appeared (see figure 12), reminiscent of the 'wedding cake' structures predicted in section 3.1 and in figures 6 and 7. From theory [58], the wedding cakes grow on the templates of the first-layer islands, and their spacing is determined by the density, N, of first-layer nuclei. In one dimension, N is given approximately by

$$N \sim (F/D)^{1/4}. \tag{3}$$

For the values in table 1, this gives a value of $N \sim 0.057$ islands per site, which predicts 17 islands for a plot of 300 horizontal sites (remembering the standard block size is 2×2). Figure 12 exhibits 15 wedding cake structures, which is remarkably consistent with the theory.

Figure 13 shows how the RMS roughness of the surface depends upon P_{desorb}. For values of $P_{\text{desorb}} > 0.01$, the RMS roughness of the surface is <3 blocks (over a grid width of 300), meaning that the surface is essentially smooth.

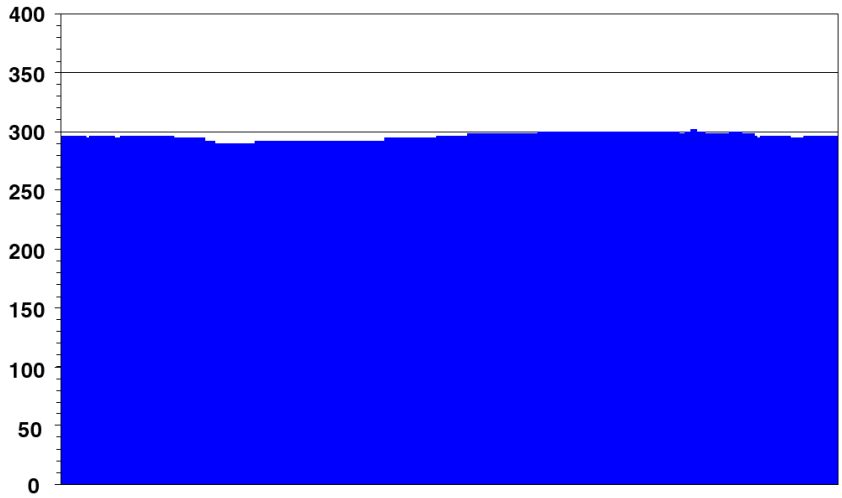

Figure 11. Simulated cross-section of a diamond film grown using the standard conditions given in table 1 but with β-scission turned off ($P_{\text{beta}} = 0$), for a 600×400 grid and blocks of size 2×2.

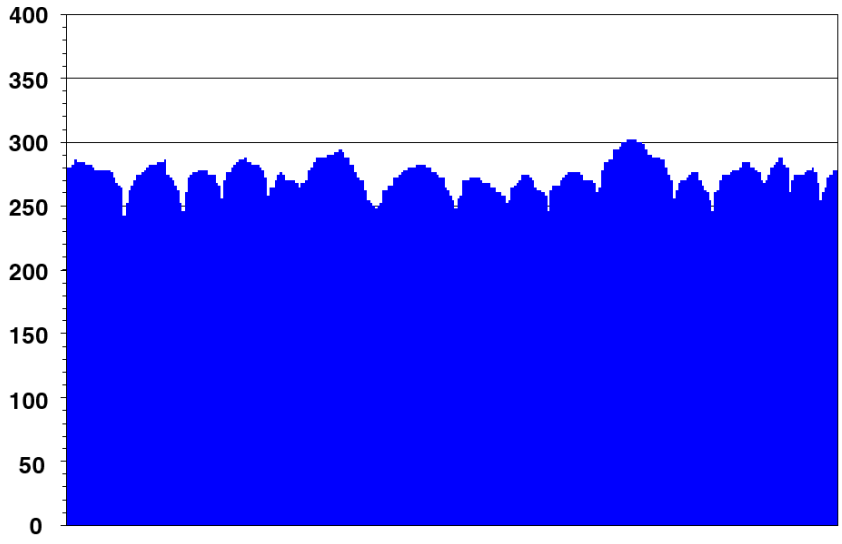

Figure 12. Simulated cross-section of a diamond film grown using same conditions as figure 11, except with $P_{\text{desorb}} = 0.005$. The rounded 'wedding cake' morphology is consistent with that shown in figure 7.

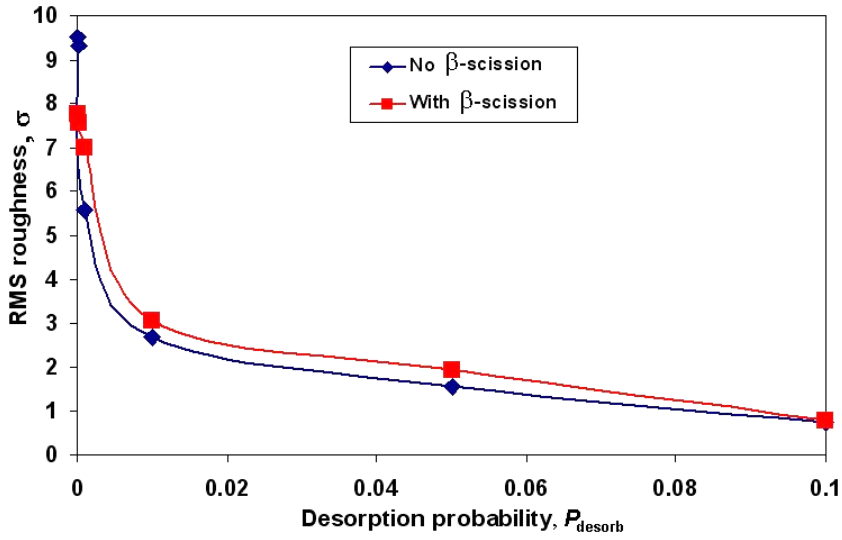

Figure 13. RMS roughness, (in blocks, where 1 block = 1 C–C bond length ∼1.5 Å) as a function of P_{desorb}, with β-scission turned on (red squares) and off (blue diamonds). All the other conditions as in table 1.

At smaller values of P_{desorb} the roughness increases, first to the wedding cake structures, and finally to a spiky, random surface such as that shown in figure 14 when $P_{\text{desorb}} < 0.005$. These types of surface should, in theory, be fractal or, more accurately, *self-affine* [60]. This means that as the film grows, the same surface structures are repeated at increasing length-scales. A self-affine surface is characterized by fluctuations in the perpendicular direction $\sigma(L)$ (i.e. the RMS roughness) which increase with the horizontal length L sampled as $\sigma(L) \propto L^H$, where $0 < H < 1$ is called the *roughness exponent* [61]. Therefore, a test for self-affinity is that a plot of $\ln\sigma$ against $\ln L$ should give a straight line of gradient H. Figure 15 shows such a plot confirming that the spiky surface from figure 14 is self-affine with $H = 0.3$. Although of fundamental interest, such spiky surfaces have never been reported in diamond CVD, therefore we can assume that values of $P_{\text{desorb}} < 0.005$ are unreasonable under CVD conditions and we shall not consider them further.

We conclude that, despite the thermodynamic arguments against carbon desorption/etching (see section 2.2), such a process must exist with an average rate consistent with a probability ∼0.05 in order to obtain the flat morphologies seen experimentally.

3.3. *Effect of β-scission (P_{beta})*

Figure 13 shows two plots, one with β-scission included in the model and one with β-scission turned off. For values of $P_{\text{desorb}} > 0.005$, where the surface is predominantly flat, the two curves lie almost on top of each other, with the small difference being mainly due to run-to-run variations as a result of the random nature of Monte Carlo simulations. Only at

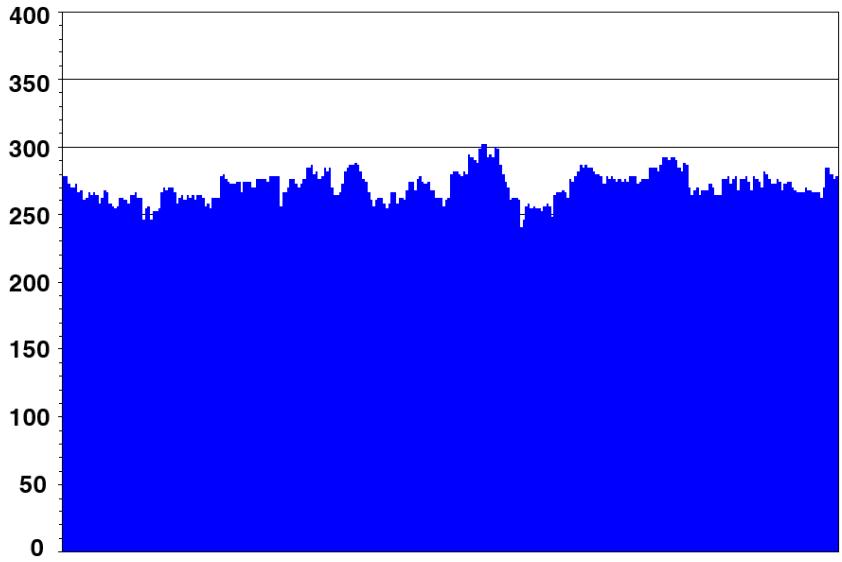

Figure 14. Simulated cross-section of a diamond film grown using the same conditions as figure 11, except with $P_{\text{desorb}} = 0$, for a 600 × 400 grid and blocks of size 2 × 2.

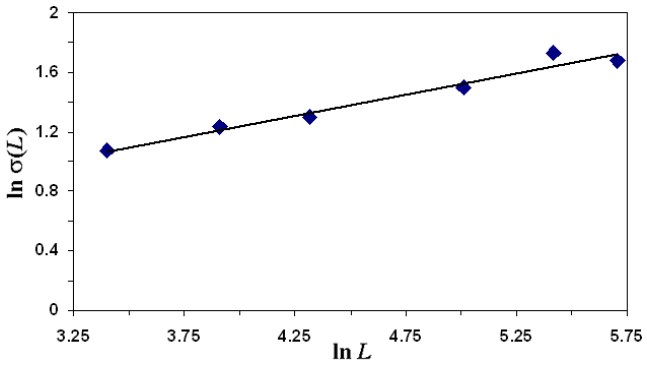

Figure 15. Log–log plot of RMS roughness $\sigma(L)$ as a function of horizontal length L over which σ was calculated (both in units of blocks, where 1 block = 1 C–C bond length ∼1.5 Å). The straight line trend indicates that this surface structure is self-affine.

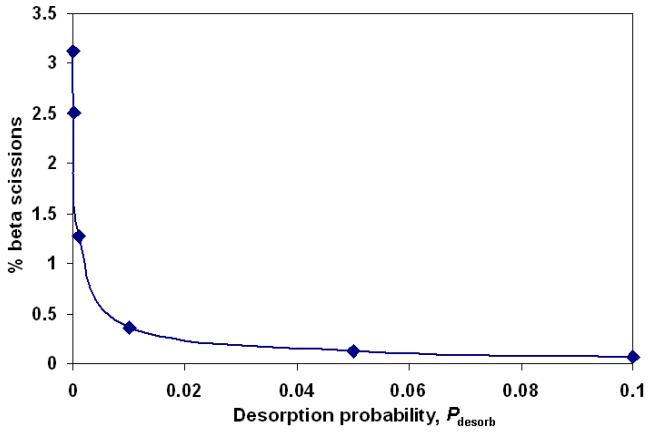

Figure 16. The percentage of β-scission reactions (relative to the total number of carbons added to the surface) as a function of P_{desorb} for the standard conditions given in table 1.

smaller (unrealistic) values of P_{desorb} does β-scission reduce the roughness significantly. Similarly, the growth rate with β-scission turned on is only slightly lower (by around 5–7%) than that with it turned off, for all values of P_{desorb}. Thus, for standard diamond CVD conditions, β-scission can be considered a relatively unimportant process when it comes to determining the growth rate and the surface roughness. Only at unrealistically small values of P_{desorb} does β-scission play a role, preventing the formation of the longest of the spikes.

This is somewhat surprising since it is generally believed [13] that β-scission is a major process responsible for keeping the surface smooth. However, a plot of the percentage β-scissions as a function of P_{desorb} (figure 16) shows that for typical CVD conditions where $P_{\text{desorb}} \sim 0.05$, only ∼0.12% (∼1-in-800) of all incoming carbon species undergo a β-scission reaction and are removed from the surface. Recall that this will be a maximum value, since the rate of β-scission reactions was taken to be equivalent to the program time-step (i.e. the same as the migration rate). The true rate for β-scission may be significantly slower than this due to considerations of the H atom flux and abstraction rate which are needed to initiate the reaction. Thus, β-scission appears to be a minor pathway compared to the other possible fates for adsorbed C species, such as etching or incorporation into the lattice. β-scission only becomes significant—with percentages >1%—at the unrealistically low values of P_{desorb} that produce the spiky surfaces.

Another interesting result from these simulations is shown in figure 17. The percentage of adsorbing carbon species which *never* jump (even with $P_{\text{mig}} = 0.67$) remains constant at a surprisingly high level of ∼16–20% for conditions which produce the smooth surfaces ($P_{\text{desorb}} > 0.005$). These carbons are those which never have the opportunity to migrate because they (i) landed directly next to a step-edge and immediately attached, (ii) temporarily adsorbed on a terrace but at the next time-step, a second, migrating carbon jumped next to

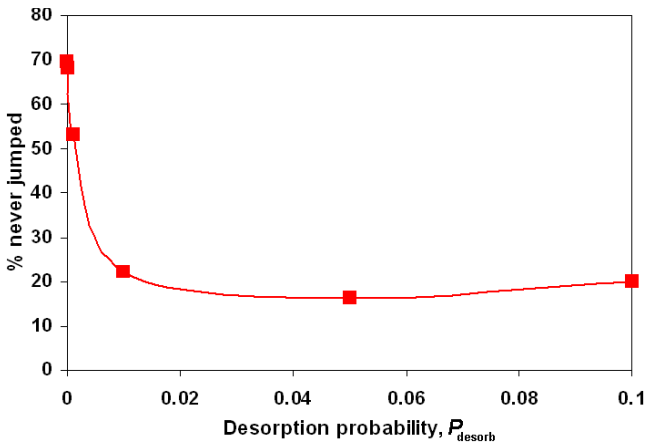

Figure 17. The percentage of adsorbing carbons (relative to the total number of carbons added to the surface) that never even jumped one time as a function of P_{desorb}, with β-scission turned on, and the conditions in table 1.

them forming a critical nucleus, or (iii) they formed a surface defect. For the values of $P_{\text{dir-def}}$ and $P_{\text{jump-def}}$ given in table 1, the percentage of surface defects created is calculated to be ∼3%. Therefore the remaining ∼17% of 'non-migrating' carbons must be due to a combination of processes (i) and (ii). Again, the curve with β-scission turned off (not shown) almost overlaps that shown in figure 17, consistent with β-scission being a relatively unimportant process.

3.4. Effect of P_{mig}

Although the program time-step was chosen with $P_{\text{mig}} = 1$, the standard value chosen for P_{mig} for most of the simulations was 0.67. This gives equal probability for the species to jump left, right, or stay in place. The effect of changing the rate of migration was studied by two methods. In the first, a loop was added to the program code to allow the migrations and processes associated with the migrating blocks (desorption, defect formation, addition to the lattice) to be repeated more often than the standard time-step. Thus, the effect of running this loop 10 times is to effectively increase the migration rate by a factor of 10, while keeping all the other rates at their standard values. However, the probabilities of the two processes occurring within the loop (P_{desorb} and $P_{\text{jump-def}}$) also need to be reduced by an amount $P_{\text{approx}} \sim P/m$ where P is the standard value of both processes from table 1 and m is the number of loops. This needs to be done in such a way that after m loops, the probability of each process having occurred at some point during the loop is identical to the standard value. Analysis of the probabilities shows that the exact probability value to be used is given by

$$P_{\text{new}} = \sum_{i=0}^{m-1} P_{\text{approx}}(1 - P_{\text{approx}})^i. \quad (4)$$

Figure 18(a) shows that the growth rate is a rather weak function of the migration rate, changing by a factor of only ∼3 while the migration rate changes over a factor of 500 (0.1–50× standard rate). Figure 18(b) shows that the RMS roughness also changes very little over this range, with the films remaining largely flat. Figure 18(c) shows that the mean number of jumps made by each migrating species is a near linear function of the migration rate, and for the faster rates n can have values of several hundred. Plotting the growth rate against the surface diffusion length ℓ_s, as in figure 18(d), gives a linear trend. This suggests that the growth rate is proportional to the diffusion length, although the dependence is relatively weak.

In comparison with the first method used to test the effect of migration rate the second method mostly tests migration rates that are slower than the standard time-step. In this method, the value of P_{mig} was simply changed from 0 to 1, while keeping all other conditions standard. The results are plotted in figure 19, which highlights, once again, that migration only makes a difference of 2–3 to the growth rates for a given desorption rate.

3.5. Effect of P_{new}

P_{new} is related to the impact rate of CH_3 species onto radical sites, and it is the balance between this parameter and P_{desorb} which governs the equilibrium between species landing on the surface to those being removed, and thus, the overall growth rate. If P_{desorb} remains constant at its standard value of 0.05, then increasing P_{new} will serve to increase the growth rate. Indeed, figure 20 shows that plotted on a log–log scale the growth rate is strongly related to P_{new}. However, this increased growth rate is accompanied by a concomitant increase in roughness, because Eley–Rideal-type growth (as seen previously in figure 3(b)) starts to dominate migration and Langmuir–Hinshelwood growth (figure 3(a)). These effects can be counteracted, of course, by changing the process conditions accordingly, such as increasing the surface temperature or altering the gas mixture. Nevertheless, all things being equal, this switch from LH to ER growth can be regarded as a rationale for the widely-reported feature of diamond growth that, in general, the 'faster it is grown, the poorer the quality'.

3.6. Effect of the renucleation probabilities, $P_{dir-def}$ and $P_{jump-def}$

First, let us examine the combined effect of both probabilities, with $P_{\text{renucl}} = P_{\text{dir-def}} = P_{\text{jump-def}} = 0.0005$, as in table 1. The effect of P_{renucl}—which can be considered as the probability of forming a surface defect by whatever mechanism—upon growth rate can be seen in figure 21 for low, medium and high values for P_{desorb}. The surface defect would act as a critical nucleus for growth, but its importance in the overall growth process depends upon the relative rates of competing processes. For convenience, we shall consider the effects of P_{renucl} at low and high values of P_{desorb} separately.

(i) *Low values of* P_{desorb}. These probability values might occur at low deposition temperatures and/or low H atom concentrations, and might be relevant to the conditions

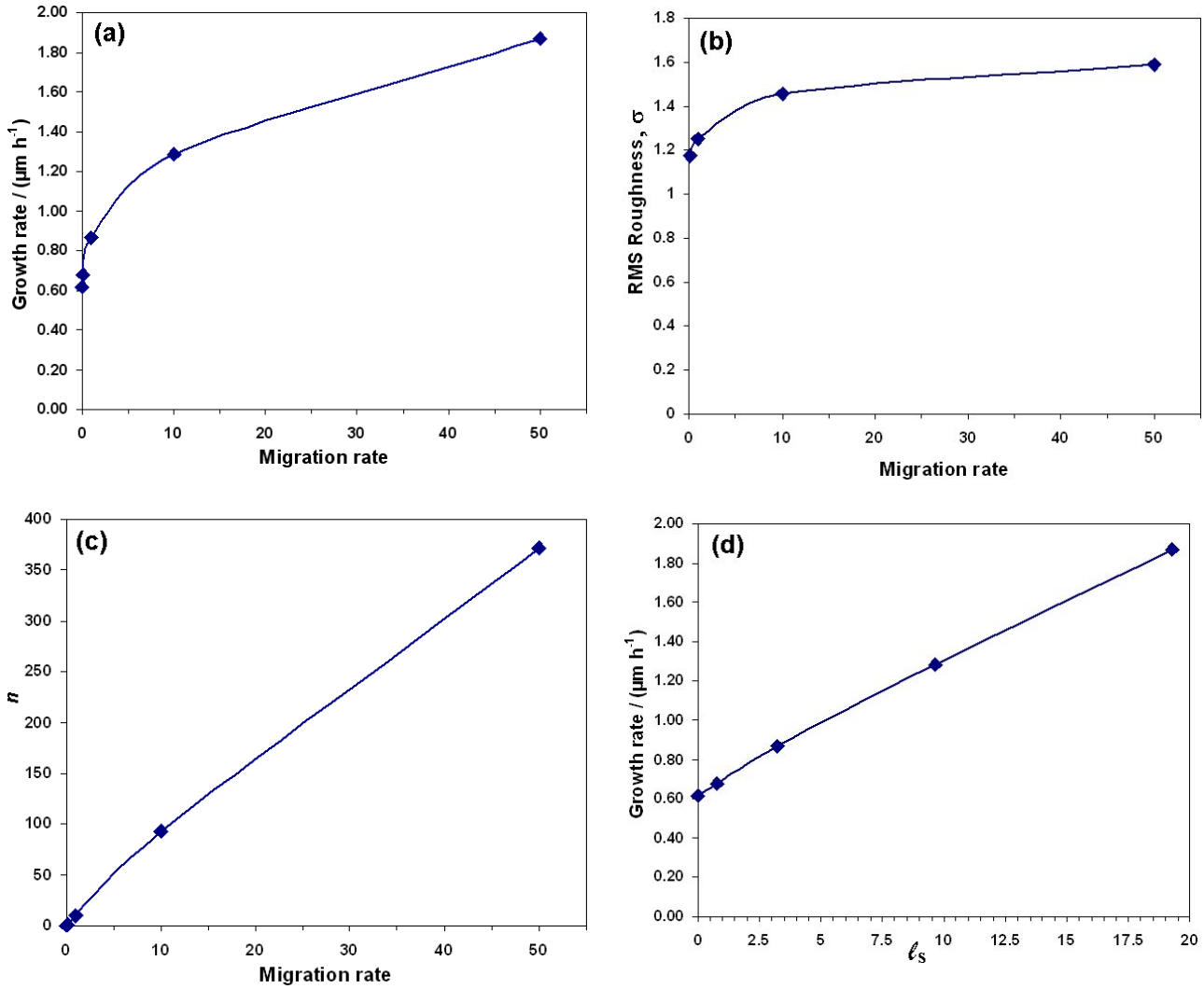

Figure 18. The variation of various film properties as a function of migration rate. The migration rate is measured in multiples of the standard rate, so a value of 10 means that the migration occurs 10× faster than the standard value given in table 1 would produce, with all other parameters the same. (a) Growth rate, (b) RMS roughness (in blocks, with 1 block = 1 C–C bond length ∼1.5 Å), and (c) the mean number of jumps made by each adsorbing block n. (d) The growth rate plotted against the diffusion length ℓ_s, with the equation of the best-fit line being: growth rate (μm h^{-1}) $= 0.0647\ell_s + 0.64$.

used for NCD growth. Under these conditions the rate-determining step for growth is simply the arrival rate of new adsorbing carbons. Since desorption/etching is slow, almost all of the carbons eventually add to the lattice in some form, and the growth rate will be close to the maximum possible, i.e. 4.3 μm h^{-1}. Even if many of these carbons do not add 'cleanly' to the lattice, but instead form surface defects, this does not appreciably affect the growth rate. Thus, we see in figure 21 that for $P_{\text{desorb}} = 0.000\,15$, the growth rate changes from 4.0 to only 4.3 μm h^{-1} even though P_{renucl} is varying over five orders of magnitude. Figure 22(a) shows that the surface roughness is a very strong function of P_{renucl}. For values of $P_{\text{renucl}} < 0.0001$, the RMS roughness is already quite high, due to the low desorption probability, and displays the rounded wedding cake structures mentioned in section 3.2. For values above this a very spiky surface develops, whose roughness remains constant at values of $P_{\text{renucl}} > 0.01$.

(ii) *High values of* P_{desorb}. These conditions might occur for high deposition temperatures and/or high H atom concentrations, and are more representative of typical diamond CVD conditions. Under these conditions, desorption/etching is relatively rapid, and carbons can only add to the lattice if they can find a suitable step-edge before they are removed back to the gas. Thus, the rate-determining step for growth is now the nucleation of a new layer, since once a critical nucleus is formed, rapid migration ensures that the layer is completed relatively rapidly. In this case, the critical nucleus will most likely be the surface defect. Figure 21 shows that the growth rate is now a strong function of P_{renucl}. For $P_{\text{desorb}} = 0.05$ changing P_{renucl} over the same five orders of magnitude as above now results in an eight-fold increase in growth rate. When P_{renucl} is small (<0.01) the growth rate is slow (because of the time involved in waiting for a surface defect to appear and create a critical nucleus), but

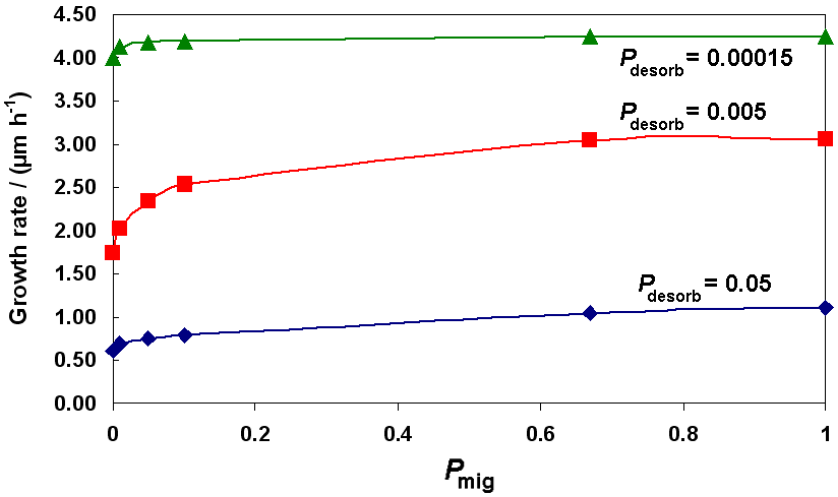

Figure 19. Growth rate plotted against P_{mig} for three different values of P_{desorb}, with all other conditions as in table 1.

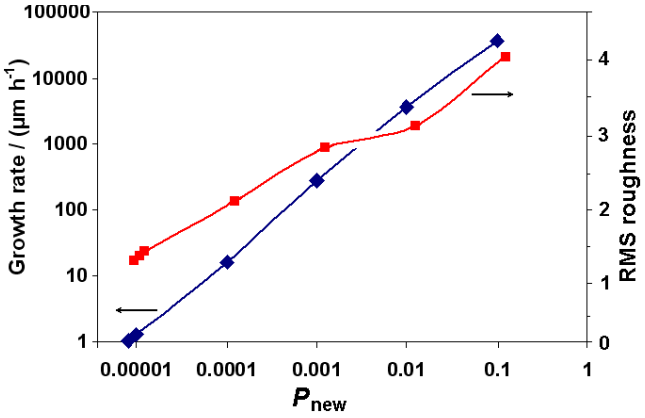

Figure 20. Growth rate (blue diamonds) and RMS roughness (red squares) in blocks (1 block = 1 C–C bond length ∼1.5 Å), plotted against the probability of choosing a new impacting CH3 group, P_{new}, with all other conditions as in table 1.

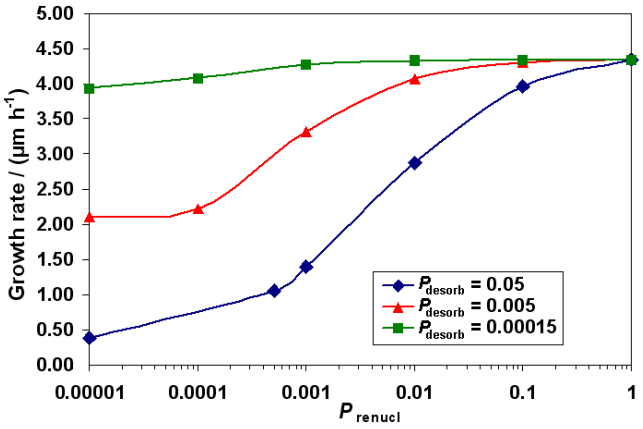

Figure 21. Growth rate as a function of P_{renucl} for three values of P_{desorb}, with all other parameters the same as those in table 1, except with β-scission off.

the resulting film is very flat since the layer growth is dominated by migration processes. Increasing P_{renucl} by a small amount now directly decreases the waiting time for the next critical nucleus, and so the growth rate increases rapidly. Figure 22(b) shows that the films are much smoother, with RMS roughness values <2 blocks for $P_{\mathrm{renucl}} < 0.05$. The roughness only becomes significant for unrealistically high values of P_{renucl}. Thus, these simulations are consistent with the observation that ppm levels of surface-active reactants (such as C atoms or CN radicals) in the gas phase cause such a significant increase in growth rate while being incorporated into the bulk in only trace amounts.

(iii) *Varying the relative values of* $P_{\mathrm{dir-def}}$ *and* $P_{\mathrm{jump-def}}$. Since the two defect-forming processes are different in nature, it is worthwhile determining the effect of giving them different probabilities. Clearly, $P_{\mathrm{jump-def}}$ is the more important parameter, since this determines the chance of creating a surface defect by every migrating block at every time-step. In contrast, $P_{\mathrm{dir-def}}$ can only determine the formation of a defect when a new block strikes the surface for the first time. The ratio of the rates of these two processes (table 1) is ∼200 000:1, so for the standard growth conditions we would expect many more defects to be created via migration than via direct adsorption. Analysis of the results shows that, for standard growth conditions (with $P_{\mathrm{dir-def}} = P_{\mathrm{jump-def}} = 0.005$), only ∼0.2% of the total number of blocks in the lattice were black-coloured blocks representing surface defects created by direct adsorption ($P_{\mathrm{dir-def}}$), while 3.2% of the lattice blocks were brown-coloured blocks representing defects created from migration processes. This ratio is much smaller than the maximum ratio of 200 000 because many of the migrating blocks desorbed or added to the lattice before they had the opportunity to form a surface defect. Therefore, as expected, creation of surface defects as a result of migration is more important in determining the growth rate and morphology than the equivalent process by direct adsorption. This can be seen in figure 23 (curve (b)), where increasing or decreasing $P_{\mathrm{dir-def}}$ by a factor

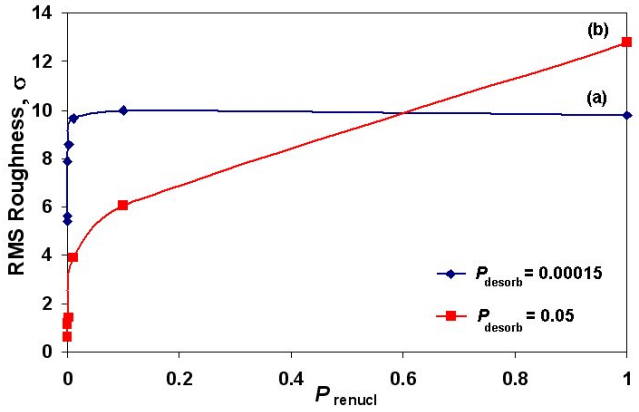

Figure 22. RMS roughness, σ (in blocks, with 1 block = 1 C–C bond length ~1.5 Å) as a function of the combined probability of forming a surface defect, P_{renucl}, with all other parameters the same as those in table 1, except with β-scission off and (a) $P_{\text{desorb}} = 0.000\,15$, (b) $P_{\text{desorb}} = 0.05$.

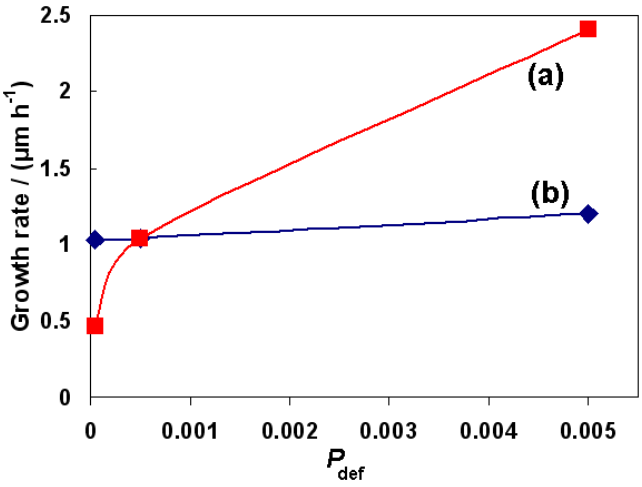

Figure 23. Growth rate plotted as a function of the probability of creating a surface defect as a result of (a) surface migration with $P_{\text{def}} = P_{\text{jump-def}}$, and (b) direct adsorption with $P_{\text{def}} = P_{\text{dir-def}}$, with the other probabilities given in table 1.

of 10 while keeping all other rates constant has very little effect upon growth rate, whereas the same change in $P_{\text{jump-def}}$ (curve (a)) affects the growth rate by a factor of ±5. Reliable values for these two probabilities, and in particular for $P_{\text{jump-def}}$, are crucial if we are to understand the diamond growth process. Again, putting these values on a firmer theoretical footing is suggested as a challenge for theoreticians.

3.7. Effect of probability of adding to a step-edge, $P_{add-step}$

In the model so far we have assumed that, upon meeting a step-edge, a migrating C species attaches permanently with no barrier to this bonding process. In the case of MBE, where the migrating species are often metal atoms, this is a reasonable assumption, since the bonding forces would be primarily electrostatic. However, for diamond, this attachment process

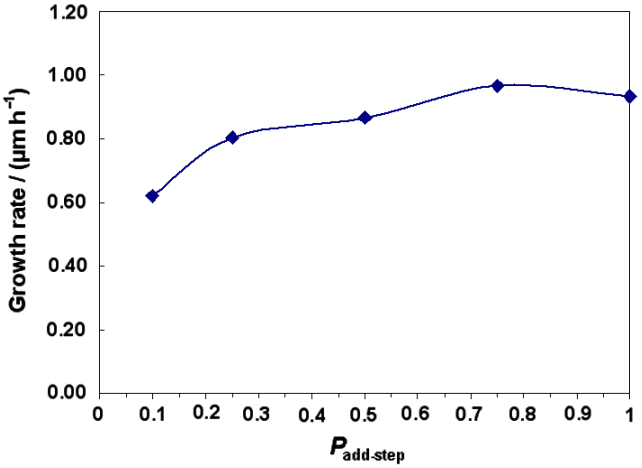

Figure 24. Growth rate plotted as a function of the probability of a migrating block attaching to a sidewall, with all other values the same as in table 1.

is not so straightforward since attachment of the migrating CH_2 group into an existing sidewall would require, at the least, some sort of surface reconstruction, as well as the breaking and making of several C–H and C–C bonds. Attachment may even require a more complicated process involving a separate reaction, such as the 'void filling' reaction proposed by Netto and Frenklach [44]. In any case, in the Monte Carlo model we can evaluate the importance of this 'sidewall sticking probability' by simply changing the probability which determines whether a migrating block attaches to a sidewall ($P_{\text{add-step}}$) from 1 to a lower value. As might be expected, figure 24 shows that the growth rate drops slightly as $P_{\text{add-step}}$ decreases. However, this decrease is relatively small until $P_{\text{add-step}}$ becomes less than ~0.1, below which the growth rates became unrealistically small. Decreasing $P_{\text{add-step}}$ from 1 to 0.1 has only a minor effect upon both RMS roughness (which remains at ~1.5 ± 1 blocks) and upon n which drops from 10.6 to 10.0 over this range. Thus, we can conclude that the main effect of decreasing $P_{\text{add-step}}$ is simply to decrease the overall growth rate without changing the overall growth mechanism. However, we note in passing that this is yet another growth parameter that needs to be more accurately evaluated by detailed quantum-mechanical or molecular-mechanical modelling.

3.8. Step bunching

Step-bunching is the formation of macro-steps (often many atomic layers high) as a result of different growth speeds at different step-edges. As the faster moving step-edges catch up with slower ones, the steps tend to aggregate (or bunch) together forming higher steps, often separated by wide terraces [62]. A number of models have been proposed for the physical origin of step-bunching, based on an asymmetry in the attachment/detachment rates of atoms at step-edges [47] or adsorbed impurities inhibiting step-growth [63]. However, in most cases of crystal growth the mechanism is still not clear. Step-bunching has been observed during diamond growth,

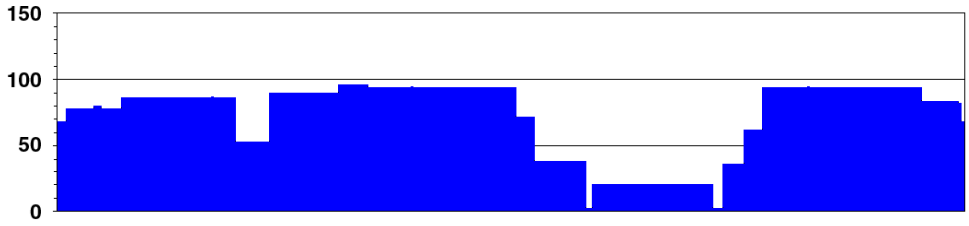

Figure 25. A qualitative simulation of step-bunching as a result of the inhibition of step movement by immobile surface defects. Rather than a relatively smooth surface consisting of a large number of atomic-scale steps (e.g. figure 11), the steps have bunched together to form macro-steps that are many 10s of blocks high.

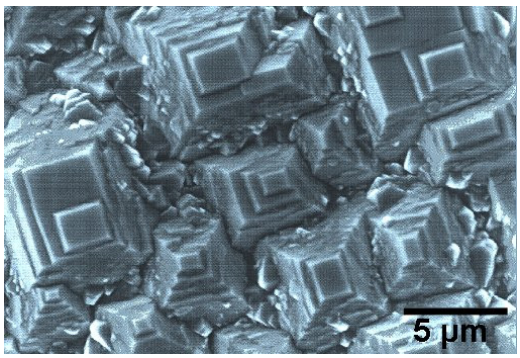

Figure 26. Macroscopic growth pyramids on the (100) diamond surface after using CH_4/H_2 and 80 ppm N_2 additions. The pyramids resemble the structures simulated in figure 25. Reprinted with permission from [67]. Copyright 1995 Elsevier.

especially at high methane content [64], low deposition temperature [22], or with additions of N_2 to the gas phase [65] (all of which are consistent with the adsorbed-impurity model). KMC modelling of step-bunching has been performed by other groups on 2D crystal surfaces [62], but is difficult to reproduce such 2D phenomena using a 1D model such as one described here. However, it is possible to test the idea of adsorbed impurities inhibiting step-growth by a simple modification to the program in which the migrating C species (green blocks) do not recognize the surface defects (black or brown blocks) as step-edges, and so do not attach to them. In this case, the immobile surface defects do not act as critical nuclei, but instead act as 'road-blocks', preventing the lateral spread of steps. However, nucleation can still occur on layers above the surface defects, but lateral spread of the layers cannot go beyond the defect due to the positive ESP barrier for migration off a step-edge. This results in the steps bunching up and coalescing to form macroscopic steps that are many 10s of blocks high (see figure 25). These macroscopic steps are qualitatively consistent with those seen experimentally (see figure 26). However, this model cannot represent step-bunching accurately because the surface defects are considered immobile, leading to fixed step-edges. In reality, a step-edge would eventually grow around the surface defect from either side, and thus the step-edge would continue to move beyond the position of the defect. Nevertheless, we have shown that some aspects of step-bunching can be duplicated even with a 1D model.

4. Conclusions

We have shown that, given reasonable values for the input parameters, a remarkably simple 1D Monte Carlo model can reproduce many of the experimentally observed features of CVD diamond growth on a (100) surface. The growth rate is determined mainly by a balance between the flux of CH_3 species to the surface and the desorption/etching rate. Using values for the various rates from the literature we estimate a growth rate for standard diamond growth conditions of $\sim$1 μm h^{-1}, which is consistent with experimental values. Migration of species along and across dimer rows is essential to obtain step-edge growth and smooth surfaces. Without migration, the surfaces become rough and spiky, and the growth rate drops typically by a factor of $\sim$2, although the exact amount depends upon the choice of conditions, and can be several times this value, if for example, a much faster migration rate is used. The growth rate enhancement caused by migration is roughly proportional to the surface diffusion length $\ell_s = \sqrt{n}$, where n is the mean number of jumps made by a migrating block. It follows that the growth rate enhancement is due to the increased probability of the migrating species meeting a step-edge due to it sampling a larger number of surface sites than a stationary species.

By using a parameter to represent random surface defect formation, growth morphologies resembling 'wedding cake' structures can be produced, which again, are consistent with atomic-scale morphologies seen experimentally, and may, in principle, be scaled up to rationalize the cauliflower or ballas diamond morphologies seen at higher C:H ratios. β-scission has been shown to be a minor process, removing only 1-in-800 of the adsorbing carbons from the lattice. Thus, its importance in maintaining a smooth growing surface and in removing longer-chained polymeric species from the surface may have been previously over-estimated.

A useful feature of a simple Monte Carlo model such as this is that it can reveal gaps in our knowledge, as well as suggest areas where more work needs to be done. In particular, we highlight the following points in order to stimulate more detailed theoretical studies.

- How many carbon atoms (or CH_x species) are required to join together on a (100) diamond surface to form the critical nucleus for nucleation of a new layer? For our 1D model we assumed either a pair of 2 'normal' carbons or a special surface defect atom are sufficient for this purpose.

But is this so for the actual diamond surface? And will this critical nucleus size be different on different surfaces?

- The desorption/etching rate for a carbon species from the surface is a vital parameter which controls the surface morphology. Using an averaged value of 77 550 s^{-1} (table 1) with $P_{desorb} \sim 0.05$ produces the smooth surfaces and growth rates consistent with those seen experimentally. However, the exact mechanism(s) by which C is removed from a diamond surface have still to be determined [56], and thus, at present, the (single) value used for the 'rate of desorption' is little more than educated guesswork.
- The same is true for the two probabilities used to model surface defects, $P_{dir-def}$ and $P_{jump-def}$. The value of $P_{dir-def}$ would depend upon the identity of the reactive adsorbate, for example atomic C, CH, or CN, and upon which type of site it was adsorbed (monoradical or biradical). We have made no attempt to distinguish between different reactive adsorbates or sites, and allocated the same probability to each. A more detailed model would need to consider each possible defect-causing species in turn, along with their relative concentrations near the surface. The value of $P_{jump-def}$ is more critical, since this is tested at every time-step, yet its value, too, is little more than an educated guess. Detailed *ab initio* calculations need to be made to ascertain what defects (if any!) are possible when a migrating CH_2 bridging group bonds 'crookedly', and of the energies associated with these defects.
- Migration of the CH_2 groups off the top of step-edges has never been treated in detail in diamond surface models. In our simple model we have assumed that only the 'cowards' scenario occurs, and the other two scenarios ('lemmings' and 'eagles') are excluded. A proper *ab initio* calculation for the possible scenarios should help to determine the relative probabilities of each of these processes. This may then help to predict more accurately the conditions needed for the onset of morphologies such as the wedding cake structures or cauliflower-type mounds.
- The exact mechanism by which a migrating CH_2 bridging group bonds to a sidewall also needs to be studied, since this would lead to a more accurate value for the sidewall sticking probability, $P_{add-step}$, which might be considerably less than the default value of 1 used in these simulations.

There are some obvious extensions to this work which we are in the process of implementing. At present, the probabilities for the various reactions and processes have independent values. In a future publication these probabilities will be related to experimental parameters, such as substrate temperature or H atom concentration. The model should then be able to make realistic predictions about the effect of different growth conditions upon the growth rate, morphology and growth mechanism in real systems.

We also intend to extend the program to include aspects of the gas-surface processes consistent with our model of diamond growth that was discussed in the Introduction and detailed in [17, 20, 21]. This would involve adding routines which differentiate between adsorption and onto and desorption/etching from monoradical and biradical sites, and for different adsorbing species. Some of these processes would be dependent upon the concentrations of gas phase H and CH_3, as well as the local gas and surface temperatures.

Another extension is to model grain formation, allowing NCD, UNCD and columnar growth structures to be predicted. This can be done by allocating random colours to the surface defects, and then allowing migrating blocks that attach to a step-edge to choose (with a given probability) to take on the colour of the edge block or the colour of the underlying block. Thus, each crystallite will be colour-coded, and the size, shape and distribution of grains in polycrystalline films can be investigated. This work will appear in a future publication [66].

Extension of the 1D cross-sectional model to a two-dimensional surface is possible, but at the expense of simplicity and speed. Nevertheless, this may then allow intrinsically 2D processes, such as step-bunching, to be modelled more accurately.

Acknowledgments

The authors wish to thank Neil Fox, Keith Rosser, Ben Truscott, Walther Schwarzacher, and Jeremy Harvey for useful discussions and suggestions. The Bristol-Moscow collaboration is supported by a Royal Society Joint Project Grant. The authors wish to thank Professors V P Godbole and Lothar Ley for permission to reproduce figures 7 and 26, respectively.

References

[1] May P W 2008 *Science* **319** 1490
[2] Prawer S and Greentree A D 2008 *Science* **320** 1601
[3] Nebel C E, Rezek B, Shin D, Uetsuka H and Yang N 2007 *J. Phys. D: Appl. Phys.* **40** 6443
[4] Koeck F A M and Nemanich R J 2009 *Diamond Relat. Mater.* **18** 232
[5] May P W 2000 *Phil. Trans. R. Soc.* A **358** 473
[6] Williams O A, Daenen M, D'Haen J, Haenen K, Maes J, Moshchalkov V V, Nesládek M and Gruen D M 2006 *Diamond Relat. Mater.* **15** 654
[7] May P W, Harvey J N, Smith J A and Mankelevich Yu A 2006 *J. Appl. Phys.* **99** 104907
[8] Gruen D M, Shenderova O A and Vul'A Ya (ed) 2005 *Synthesis, Properties and Applications of Ultrananocrystalline Diamond* (*NATO Science Series Part II* vol 192) (Berlin: Springer)
[9] Bogdan G, De Corte K, Deferme W, Haenen K and Nesládek M 2006 *Phys. Status Solidi* a **203** 3063
[10] Isberg J, Hammersberg J, Johansson E, Wikström T, Twitchen D J, Whitehead A J, Coe S E and Scarsbrook G A 2002 *Science* **297** 1670
[11] Yan C-S, Li H-K, Mao W, Qian J, Zhao Y and Hemley R J 2004 *Phys. Status Solidi* a **201** R25
[12] Ho S S, Yan C S, Liu Z, Mao H K and Hemley R J 2006 *Indust. Diamond Rev.* **66** 28
[13] Goodwin D G and Butler J E 1998 *Handbook of Industrial Diamonds and Diamond Films* ed M A Prelas, G Popovici and L K Bigelow (New York: Dekker)
[14] Harris S J 1990 *Appl. Phys. Lett.* **56** 2298
[15] Butler J E and Oleynik I 2008 *Phil. Trans. R. Soc.* A **366** 295
[16] Das D and Singh R N 2007 *Int. Mater. Rev.* **52** 29

[17] May P W and Mankelevich Yu A 2008 *J. Phys. Chem.* C **112** 12432
[18] Skokov S, Weiner B and Frenklach M 1994 *J. Phys. Chem.* **98** 7073
[19] Richley J C and Ashfold M N R 2009 in preparation
[20] May P W, Ashfold M N R and Mankelevich Yu A 2007 *J. Appl. Phys.* **101** 053115
[21] Mankelevich Yu A and May P W 2008 *Diamond Relat. Mater.* **17** 1021
[22] Lee N and Badzian A 1997 *Diamond Relat. Mater.* **6** 130
[23] Skokov S, Weiner B and Frenklach M 1994 *J. Phys. Chem.* **98** 8
[24] Thiel P A and Evans J W 2000 *J. Phys. Chem.* **104** 1663
[25] Skokov S, Weiner B and Frenklach M 1995 *J. Phys. Chem.* **99** 5616
[26] Skokov S, Weiner B, Frenklach M, Frauenheim T and Sternberg M 1995 *Phys. Rev.* B **52** 5426
[27] Frenklach M and Skokov S 1997 *J. Phys. Chem.* B **101** 3025
[28] Cheesman A 2006 Investigations into the fundamentals of gas-phase and gas-surface chemistry prevalent in growth of chemical vapour deposited diamond films *PhD Thesis* School of Chemistry, Bristol University, UK July
[29] Cheesman A, Harvey J N and Ashfold M N R 2008 *J. Phys. Chem.* A **112** 11436
[30] van Enckevort W J P, Janssen G, Vollenberg W, Schermer J J, Giling L J and Seal M 1993 *Diamond Relat. Mater.* **2** 997
[31] Frenklach M, Skokov S and Wiener B 1994 *Nature* **372** 535
[32] Frenklach M and Wang H 1991 *Phys. Rev.* B **43** 1520
[33] Harris S J and Goodwin D G 1993 *J. Phys. Chem.* **97** 23
[34] Coltrin M E and Dandy D S 1993 *J. Appl. Phys.* **74** 5803
[35] Yu B W and Girschick S L 1994 *J. Appl. Phys.* **75** 3914
[36] Frenklach M 1992 *J. Chem. Phys.* **97** 5794
[37] Clark M M, Raff L M and Scott H L 1995 *Phys. Rev.* B **54** 5914
[38] Dawnkaski E J, Srivastava D and Garrison B J 1996 *J. Chem. Phys.* **104** 5997
[39] Battaile C C, Srolovitz D J and Butler J E 1997 *J. Appl. Phys.* **82** 6293
[40] Battaile C C, Srolovitz D J, Oleinik I I, Pettifor D G, Sutton A P, Harris S J and Butler J E 1999 *J. Chem. Phys.* **111** 4291
[41] Angus J C, Sunkara M K, Sahaida S R and Glass J T 1992 *J. Mater. Res.* **7** 3001
[42] Mani R C and Sunkara M K 2003 *Diamond Relat. Mater.* **12** 324
[43] Battaile C C and Srolovitz D J 2002 *Annu. Rev. Mater. Res.* **32** 297
[44] Netto A and Frenklach M 2005 *Diamond Relat. Mater.* **14** 1630
[45] Pimpinelli A and Villain J 1998 *Physics of Crystal Growth* (Cambridge: Cambridge University Press)
[46] Ehrlich G and Hudda F G 1966 *J. Chem. Phys.* **44** 1039
[47] Schwoebel R L 1968 *J. Appl. Phys.* **40** 614
[48] Boudart M and Djéga-Mariadassou G 1984 *Kinetics of Heterogeneous Catalytic Reactions* (Princeton, NJ: Princeton University Press)
[49] May P W and Mankelevich Yu A 2006 *J. Appl. Phys.* **100** 024301
[50] Cao G, Schermer J, van Enckevort W J P, Elst W and Giling L 1996 *J. Appl. Phys.* **79** 1357
[51] Lecher R, Wild C, Herres N, Behr D and Koidl P 1994 *Appl. Phys. Lett.* **65** 34
[52] May P W, Burridge P R, Rego C A, Tsang R S, Ashfold M N R, Rosser K N, Tanner R E, Cherns D and Vincent R 1996 *Diamond Relat. Mater.* **5** 354
[53] Samlenski R, Haug C, Brenn R, Wild C, Locher R and Koidl P 1995 *Appl. Phys. Lett.* **67** 2798
[54] Van Regemorter T and Larsson K 2008 *Chem. Vapor Depos.* **14** 224
[55] Krug J 1997 *J. Stat. Phys.* **87** 505
[56] Butler J E, Cheesman A and Ashfold M N R 2009 Recent progress in the understanding of CVD growth of diamond *CVD Diamond for Electronic Devices and Sensors* ed R S Sussmann (Chichester: Wiley) chapter 5, pp 103–24
[57] Foord J S, Loh K P and Jackman R B 1998 *Surf. Sci.* **399** 1
[58] Michely T and Krug J 2004 *Islands, Mounds and Atoms, Patterns and Processes in Crystal Growth Far from Equilibrium* (Berlin: Springer)
[59] Godbole V P, Sumant A V, Kshirsagar R B and Dharmadhikari C V 1997 *Appl. Phys. Lett.* **71** 2626
[60] Krim J and Palasantzas G 1995 *Int. J. Mod. Phys.* B **9** 599
[61] Krim J and Indekeu J O 1993 *Phys. Rev.* E **48** 1579
[62] Kandel D and Weeks J D 1994 *Phys. Rev.* B **49** 5554
[63] Frank F C 1958 *Growth and Perfection of Crystals* ed R Doremus, B Roberts and D Turnbull (New York: Wiley) p 411
[64] Achard J, Tallaire A, Sussmann R, Silva F and Gicquel A 2005 *J. Cryst. Growth* **284** 396
[65] de Theije F K, Schermer J J and van Enckevort W J P 2000 *Diamond Relat. Mater.* **9** 1439
[66] May P W, Allan N L, Richley J C, Ashfold M N R and Mankelevich Yu A 2010 *Diamond Relat. Mater.* submitted
[67] Janischowsky K, Stammler M and Ley L 1999 *Diamond Relat. Mater.* **8** 179